

# REVIEW OF THE MAXUS 8 SOUNDING ROCKET EXPERIMENT TO INVESTIGATE SOLIDIFICATION IN A TI-AL-NB ALLOY

R. Mooney<sup>(1)</sup>, D. Browne<sup>(2)</sup>, O. Budenkova<sup>(3)</sup>, Y. Fautrelle<sup>(3)</sup>, L. Froyen<sup>(4)</sup>, A. Kartavykh<sup>(5)</sup>,  
S. McFadden<sup>(1)</sup>, S. Rex<sup>(6)</sup>, B. Schmitz<sup>(7)</sup>, D. Voss<sup>(8)</sup>

<sup>(1)</sup>Dublin Institute of Technology, Bolton St, Dublin 1, Ireland, Email: robin.mooney@mydit.ie, shaun.mcfadden@dit.ie

<sup>(2)</sup>University College Dublin, Belfield, Dublin 4, Ireland, Email: david.browne@ucd.ie

<sup>(3)</sup>EPM/SIMAP, Grenoble, France, Email: olga.budenkova@gmail.com, yves.fautrelle@simap.grenoble-inp.fr

<sup>(4)</sup>Katholieke Universiteit Leuven, Leuven, Belgium, Email: ludo.froyen@mtm.kuleuven.be

<sup>(5)</sup>Institute of Chemical Problems for Microelectronics (ICPM), Moscow, Russia, Email: karta@korolev-net.ru

<sup>(6)</sup>ACCESS e.V., Aachen, Germany, Email: s.rex@access.rwth-aachen.de

<sup>(7)</sup>EADS Astrium, Airbus-Allee 1, Bremen, Germany, Email: burkhard.schmitz@astrium.eads.net

<sup>(8)</sup>European Space Agency/ESTEC, Noordwijk, The Netherlands, Email: daniela.voss@esa.int

## ABSTRACT

A review of the MAXUS 8 sounding rocket microgravity experiment to investigate solidification structures in a Ti-Al-Nb intermetallic alloy is presented. The experiment was part of the Intermetallic Materials Processing in Relation to Earth and Space Solidification (IMPRESS) EU FP6 project. Key objectives were to investigate columnar and equiaxed solidification, and to achieve Columnar-to-Equiaxed Transition (CET) in the alloy. A microgravity experiment was designed to achieve this using a controlled power-down method. Two alloys were tested: one inoculated with a grain refiner and the other without grain refinement. Unrefined samples displayed axial and radial columnar growth. Boride inoculated samples displayed an equiaxed structure. No clear CET was achieved. The design, details, and results of the experiment are presented.

## 1. INTRODUCTION

The IMPRESS project was set up with the objective of gaining a better understanding of material processing, structure, and final properties of intermetallic alloys. One focus of the project was to develop and test TiAl based turbine blade castings. This material was selected for investigation because of its excellent mechanical properties at high temperatures and relatively low density. The material has potential to replace nickel superalloy turbine components [1]. However, TiAl alloys are difficult to process due to a very high liquidus temperature and high reactivity of molten Ti. Other problems encountered during casting are misrun, surface shrinkage, and hot tearing [2]. Overall, the aim is therefore to optimise the melting technique and casting process for industry to achieve high-quality, cast turbine blades.

Microgravity experiments offer a unique opportunity to study the effect of gravity on solidification. In microgravity the effects of convection (thermal and solutal) are minimised and subsequently

phenomenon associated with convection like sedimentation and macro-segregation, due to fluid flow, are therefore removed. By performing identical ground based experiments and comparing results it is possible to examine the effects of gravity induced fluid flow in solidification; this in turn will help to refine theoretical models of ground solidification.

One possible event in casting is Columnar to Equiaxed Transition (CET). This occurs during columnar growth when equiaxed grains begin to form, grow, and subsequently stop the columnar growth. Normally either a columnar or equiaxed grain structure is desired in industry applications, so that consistent mechanical properties are achieved throughout the casting. Directionally solidified turbine blades are the classic industry example where columnar grains are required to reduce creep at high temperature. Whereas equiaxed grain structures are preferred for applications where strength is important or to reduce susceptibility to hot tearing in castings due to poor feeding. Therefore, understanding the conditions that produce a CET is of great importance so that it can be avoided as necessary.

This paper describes the experiment design, operation, and results from the MAXUS-8 sounding rocket module TEM03-5M, where over twelve minutes (735seconds) of micro-gravity conditions was achieved.

## 2. LITERATURE REVIEW

Solidified metals form grains during solidification. Once nucleated, grains will either grow unidirectionally opposing the direction of heat flow and are termed columnar grains, or they form in the undercooled liquid ahead of the columnar solidification front and are termed equiaxed grains. The grain structure type; columnar, equiaxed, or mixed will depend on the solidification parameters. Where both grain structures are present a casting is said to have a CET. This occurs where columnar grain growth ceases due to the growth of, and subsequent impingement with, equiaxed grains. In a section of a cast component

columnar grains can be identified as having a preferred orientation that is parallel to the direction of heat flow and a crystallographic orientation that is elongated. Equiaxed grains on the other hand display a random pattern. There may be a region in a sample where the pattern is mixed. The region between columnar and equiaxed grains is the CET. A detailed account of the importance of this phenomenon to research in solidification of alloys was given by Spittle [3].

It is possible to analytically predict the conditions that will generate CET in a steady state directional solidification situation (using a Bridgeman furnace) given key solidification parameters, i.e. thermal gradient,  $G$ , and pulling velocity,  $V$ , as shown by Hunt [4]. A diagram of pulling velocity versus thermal gradient is produced and characterises the grain structure achieved into regions of columnar, equiaxed, or mixed. It should be noted that this method is specific to steady state solidification. However, the Hunt method is sometimes applied to transient (non-steady) scenarios like is a casting. For a given material the Hunt diagram can be used to identify the likely solidification path for a casting and the corresponding required values of pulling velocity and thermal gradient. The extent of undercooling,  $\Delta T$ , is related directly to the pulling velocity therefore we can attempt to design a transient solidification experiment using these criterion to give a CET for a specific material.

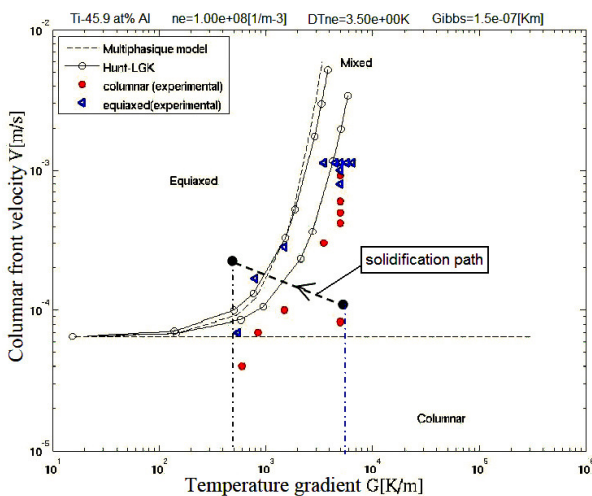


Figure 1. Hunt diagram showing a map in  $G$ - $V$  space (solidification front velocity,  $V$ , versus temperature gradient,  $G$ ) with the solidification path used to design the MAXUS-8 experiment settings shown, after [5].

A detailed account of the development of the MAXUS-8 solidification experiment was given by Lemoisson et. al. [5]. The parameters for solidification were determined according to the Hunt method. A ‘solidification path’ was identified to produce a CET in a Ti-45%at.Al binary alloy – Fig 1. The solid line and dashed lines are given by numerical modelling. The

unconnected data points were determined by Gabalcova and Lapin [6] by carrying out several directional solidification experiments and analysing the resulting grain structure. The diagram shows that a thermal gradient of 7000K/m promotes a columnar solidification structure while a thermal gradient of 500K/m will give an equiaxed structure. The experiment would have to achieve these temperature gradients and replicate the corresponding pulling velocities in order to achieve a CET.

A detailed study of the thermodynamic description for the TiAl alloy was carried out by Witusiewicz et. al [7] by using the CALPHAD (Computer Coupling of Phase Diagrams and Thermochemistry) approach and by comparing to experimental data for validation. From the phase diagram determined it is clear that TiAl alloys containing 46%at.Al solidify in a peritectic manner.

### 3. FURNACE OPERATION AND DESCRIPTION

The furnace design was similar to that used in the MAXUS-7 flight where CET in Al-Si alloys was investigated, as detailed by Sturz [8]. The new furnace design had to be capable of coping with TiAl. Changes had to be made given a different set of thermo-physical properties for the new material. The main challenges were the high liquidus temperature of the alloy and the problems due to the reactivity of molten Ti.

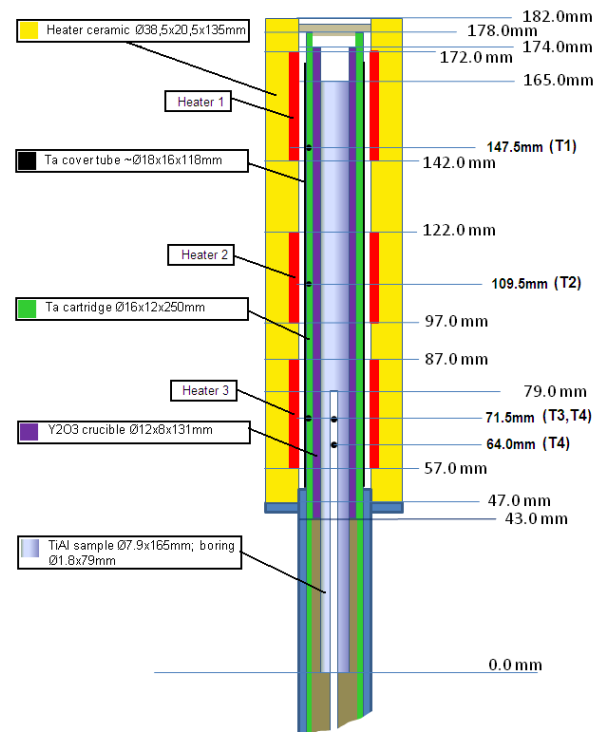


Figure 2. MAXUS-8 TEM03-5M Furnace sample configuration

The MAXUS-8 module (TEM 03-5M) was manufactured and commissioned by EADS Astrium, details here are taken from their Flight Implementation Plan for the module [9]. The module contained four integrated furnaces working independently of each other. Fig. 2 shows a schematic of the furnace configuration with dimensions. Each furnace was equipped with three in-line resistance heaters. The alloy sample ( $\varnothing 7.9\text{mm}$ ) was enclosed in a Yttrium Oxide ( $\text{Y}_2\text{O}_3$ ) crucible, wrapped in a Tantalum sleeve, and outer Tantalum cartridge. Detailed experimental research was conducted to choose the crucible material and Yttrium Oxide was determined as most suitable for handling the high temperature molten alloy. The cartridge was gastight and separated from the heater compartment by Helium so that the possibility of oxygen contamination was eliminated. The heater compartment was Argon filled. For reasons of mechanical stability and robustness, in the highly accelerated sounding rocket flight, the module had no moving parts.

Two samples of Ti-Al-Nb were tested in the experiment. One refined with Boron refiner and one without grain refinement, see Tab. 1. Furnace A and C contained the unrefined samples and furnace B and D contained the samples inoculated with Boron.

Table 1. Experiment details for Furnaces A, B, C, & D showing alloy composition, initial sample temperature settings, and cooling rates.

Furnace	A	B	C	D
Alloy (at. %)	Unrefined (Ti-45.5Al-8Nb)	Refined (Ti-44Al-7.5Nb-2.5B)	Unrefined (Ti-45.5Al-8Nb)	Refined (Ti-44Al-7.5Nb-2.5B)
Initial Sample Temperatures				
$T1$	1605°C	1555°C	1605°C	1555°C
$T2$	1580°C	1530°C	1580°C	1530°C
$T3$	1465°C	1415°C	1465°C	1415°C
Nominal Cooling Rates				
Phase I	-18K/min for 60s	-18K/min for 50s	-18K/min for 60s	-18K/min for 50s
Phase II	-36K/min for 100s	-36K/min for 40s	-36K/min for 100s	-36K/min for 40s

Each furnace had three thermocouples measuring temperatures  $T1$ ,  $T2$ , and  $T3$  fixed into the tantalum cartridge at positions shown adjacent to the heater positions in Fig. 3. One other thermocouple was fitted to measure temperature along the axis of the sample ( $T4$ ). This thermocouple position differed between the furnaces and is given by the two black dots along the sample axis in Fig 3. In furnaces A and D  $T4$  was at 64mm and in furnaces B and C  $T4$  was at 71.5mm.

There were a number of important requirements that the experiment had to satisfy. Firstly, the furnace had

to be capable of melting the sample and superheating the liquid. This was achievable as the heaters were capable of reaching a maximum temperature of 1700°C. The sample had to be directionally solidified in accordance with the solidification path as given by the Hunt diagram in Fig. 1, i.e. giving the required temperature gradient,  $G(t)$ , and front velocity,  $V(t)$ , to achieve a CET. This was realised by controlling the heaters, using a so called Power-Down technique, so that they cool at the same rate and applying specific set-point temperatures to give the required temperature gradients between heaters. Fig. 3 illustrates this method. The axial temperature gradients  $G1$  (between  $T1$  and  $T2$ ) and  $G2$  (between  $T2$  and  $T3$ ) were maintained whilst reducing the overall axial temperature with time during solidification. This was carried out in two phases as per the cooling rates given in Tab. 1.

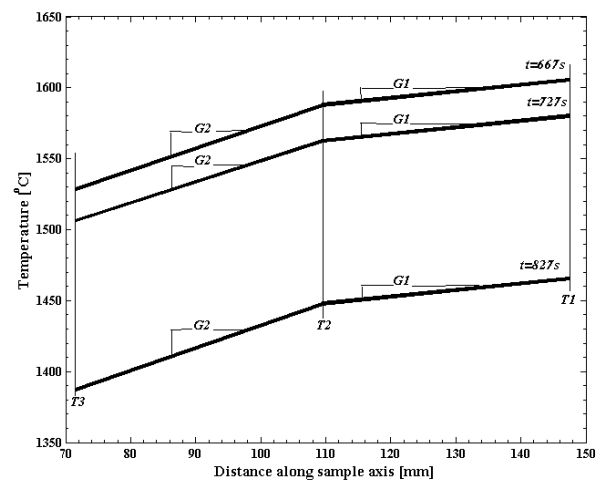


Figure 3. Schematic of Power-down technique

The sample length had to be sufficient for a CET to occur. While the sample was 160mm long the actual processed sample length was 50mm, this was considered ample from simulations carried out pre-launch. The time for solidification had to be within the microgravity state duration of the sounding rocket (12mins). Macroscale enthalpy modelling of the solidification was performed by Kartavykh et. al. [10] to show that a time of approximately nine mins would be required which was well within the microgravity time window.

#### 4. FLIGHT RESULTS

The thermal history for furnace A (unrefined sample) is shown in Fig. 4. The temperature recorded at each of the four thermocouples is plotted against time from launch of the MAXUS-8 sounding rocket. Note;  $t=0$  is the time at lift-off of the rocket. The sample was brought up to the required initial starting temperature before launch and held at this temperature for approximately ten minutes. This time allowed for any convection induced by the launch to dissipate. Then at  $t=667$ seconds phase I

of cooling begins, at  $t=727$  seconds the cooling rate doubles in phase II of cooling, and by  $t=827$  seconds the solidification is complete and all heaters are switched off.

Similarly, Fig. 5 shows the thermal history for furnace B (grain refined sample). The peak temperature for furnace B was reduced to prevent the inoculant particles from melting. Furnaces C and D carried an identical experiment set up as furnaces A and B respectively, however their results are not shown here.

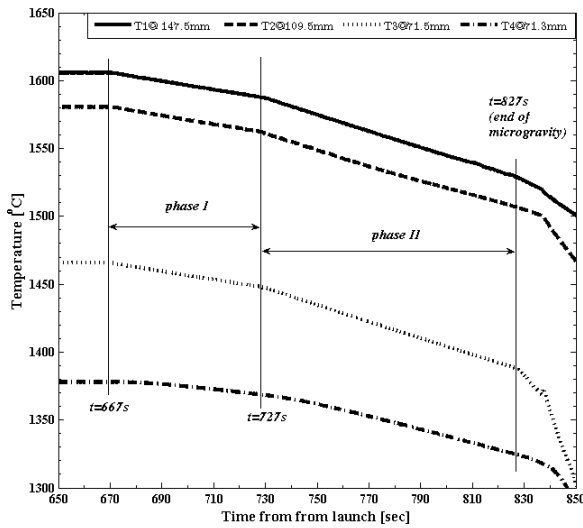


Figure 4. Thermal history of furnace A (unrefined sample)

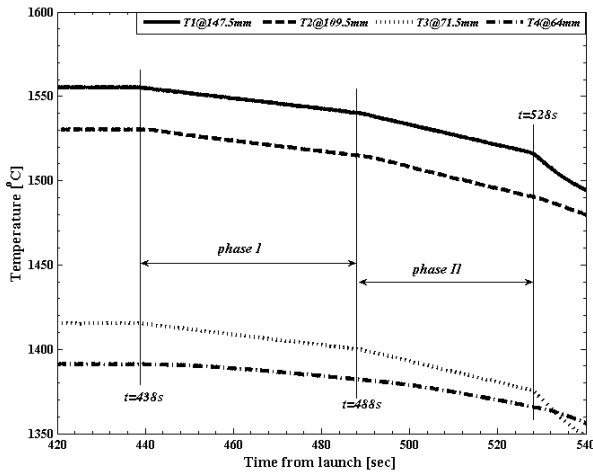


Figure 5. Thermal history of furnace B (grain refined sample)

Fig. 6 shows an image of the centre cut samples from furnace A and furnace B with the processed region shown. It should be noted that the mushy and liquid regions were restricted to the right hand side of the samples in Fig. 6, at distances greater than 100mm. The thermocouple located in the sample axis ( $T_4$ ) would never be in direct contact with the molten alloy.

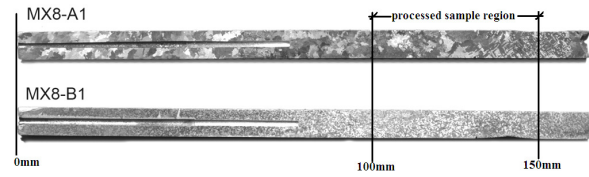


Figure 6. Image of cut samples from furnace A (non-grain refined), and furnace B (grain refined) with processed region shown.

A detailed microstructure analysis was carried out by scanning electron microscope (SEM). Fig. 7 and Fig. 8 show micrographs of the non-grain refined and grain refined samples respectively.

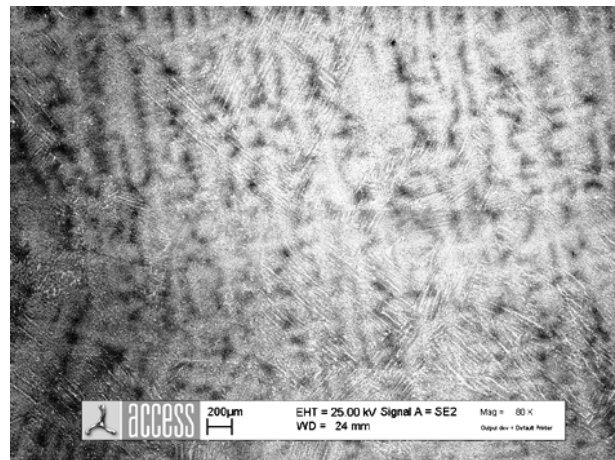


Figure 7. Micrograph of sample from furnace A, unrefined sample (Ti-45.5%at.Al-8%at.Nb)

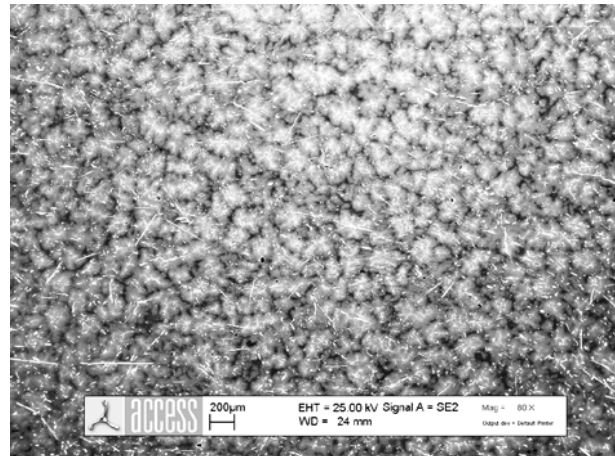


Figure 8. Micrograph of sample from furnace B, grain refined sample (Ti-44%at.Al-7.5%at.Nb-2.5%at.B)

## 5. DISCUSSION OF RESULTS

The discussion is divided into two sections; section 5.1 deals with the results from the unrefined samples, and section 5.2 discusses the refined sample results.

## 5.1 Unrefined Samples

The unrefined samples displayed a columnar dendrite growth pattern. Initially, the columnar growth is in the axial direction. Fig. 7 shows the dendrites (white elongated shapes) running from top to bottom of the figure in the same orientation as the sample axis. This behavior was expected. However, further along the sample the columnar growth begins to grow radially and eventually this growth pattern dominates the axial columnar growth at approximately 120mm along the sample. A V-shape pattern emerges at this point as shown in Fig. 9. There was no CET achieved in the unrefined samples.

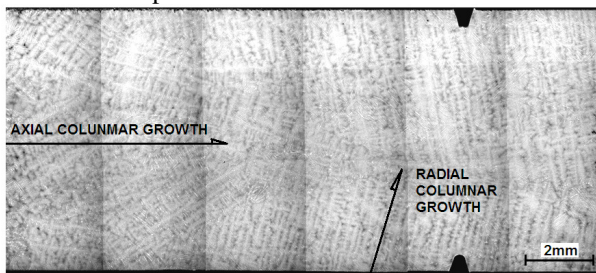


Figure 9. Micrograph showing axial and radial columnar growth in an unrefined sample (furnace A)

## 5.2 Refined Samples

In the samples refined with Boride particles the resulting grain structure was fully equiaxed. The added refiner has the effect of providing a large number of sites for heterogeneous nucleation of bcc  $\beta$ (Ti), consequently preventing columnar growth. The equiaxed dendrites form a random pattern, as clearly shown in Fig. 8. Boride particles are TiB monoborides with orthorhombic crystal structure (oP8, Pnma) grown as thin rods. Image analysis from the refined samples led to estimated average dimensions for these particles of; radius=2.5 $\mu$ m and length=50 $\mu$ m. The projected density of active TiB particles in the sample was in the range;  $1 \times 10^{10}$  to  $5 \times 10^{10} / \text{m}^3$ .

## 6. CONCLUSION AND FUTURE WORK

Firstly, it should be noted that the TEM03-5M module is capable of processing TiAl-based alloys with liquidus temperature  $T_L \sim 1500$ - $1570^\circ\text{C}$  in microgravity. This point is notable due to the extremely high liquidus temperature of the alloy and the volatile nature of molten Titanium.

There was no CET achieved in the unrefined samples. The grain refined samples produced a fully equiaxed structure throughout the sample due to the large number of sites for heterogeneous nucleation. Modeling of dendrite growth conditions and undercooling levels in the liquid alloy will help to further explain the observed results.

A significant amount of work has been completed and is ongoing to numerically model the solidification of this alloy system. McFadden and Browne [11] have developed an axis-symmetric front tracking macro-scale model to predict the solidification macrostructure and CET for diffusion controlled solid growth, i.e. for microgravity conditions. The experiment results presented here can be used to verify this model. The model can then be used as a key tool for future experiment design.

Other modeling work that has been completed on previous MAXUS sounding rocket experiments like that of Noepfel, Budenkova et. al. [12] can now be adapted to suit the MAXUS-8 flight experiment. This will add to the understanding of the solidification of this alloy system. A recent study carried out by Kartavykh et. al. [13] models the solidification of the same alloy system at the macro-scale in 2-D. Here the convection effect on solidification for terrestrial based experiments, using the same furnace module, is considered. Convection related phenomenon in solidification can then be better understood by comparing with results from this microgravity experiment.

Some furnace re-design could be considered for further similar experiments so that a CET is achieved. For example, the distance between heaters 1 and 2 could be decreased thereby reducing the potential of unwanted radial columnar growth. Also a greater sample diameter may encourage a CET.

The origin of equiaxed grains is a potential area for future research in the context of this experiment. Understanding the mode of nucleation of equiaxed grains is critical to predict a CET. Further work on this area would be useful.

Finally, the work presented provides unique benchmark data for further MAXUS sounding rockets experiments concerning solidification. It is envisaged that the work completed will lead to an enhanced experiment set up for consideration in the MAXUS-9 rocket launch scheduled for spring 2013.

## ACKNOWLEDGEMENTS

The authors would like to thank the European Commission for funding the IMPRESS research project under the EU FP6 framework, and also the European Space Agency for co-funding and co-ordinating the project. Also the Swedish Space Corporation should be acknowledged for their contribution in launching the MAXUS-8 sounding rocket.

## REFERENCES

1. Jarvis D.J., Voss D. (2005). IMPRESS Integrated Project—An overview paper, *Materials Science and Engineering: A*. Vol. 413-414, 583-591.

- 
2. Wang H., Djambazov G., Pericleous K. A., Harding R. A., Wickins M. (2009). Modeling of the Tilt-Casting Process for the Tranquil Filling of Titanium Alloy Turbine Blades. In *Proceedings of the Modeling of Casting, Welding, and Advanced Solidification Processes – XII*, Canada.
  3. Spittle J.A. (2006). Columnar to equiaxed transition in as solidified alloys. *International Materials Review*. **Vol. 51(4)**, 247–269.
  4. Hunt J.D. (1984). Steady State Columnar and Equiaxed Growth of Dendrites and Eutectic, *Materials Science and Engineering*. **Vol. 65**, 75–83, 1984.
  5. Lemoisson F., McFadden S., Rebow M., Browne D., Froyen L., Voss D., Jarvis D.J., Kartavykh A.V., Rex S., Herfs W., Grothe D., Lapin J., Budenkova O., Etay J., Fautrelle Y. (2010). The Development of a Microgravity Experiment Involving Columnar to Equiaxed Transition for Solidification of a Ti-Al Based Alloy. *Materials Science Forum*. **Vol. 649**, 17-22.
  6. Gabalcova Z., Lapin J. (2007). Columnar dendritic growth and columnar to equiaxed transition in intermetallic Ti-45.9Al-8Nb alloy. In *Proceedings European Congress and Exhibition on Advanced Materials and Processes, Euromat 2*. Nurnberg, Germany.
  7. Wtusiewicz V.T., Bondar A.A., Hecht U., Rex S., Velikanova T.Y. (2008). The Al–B–Nb–Ti system III. Thermodynamic re-evaluation of the constituent binary system Al–Ti. *Journal of Alloys and Compounds*. **Vol. 465**, 64-77.
  8. Sturz L., Zimmerman G. (2007). Microgravity experiments on columnar – equiaxed transition in Al based alloys. *International Journal of Cast Metals*. **Vol. 20**, No.3, 122-126.
  9. EADS-Astrium (2010) MAXUS-8 Flight Implementation Plan for Module TEM 03-5M.
  10. Kartavykh A., Ganina S., Grothe D., Lemoisson F., Herfs W. (2010). Numerical Simulation of TiAl-Nb alloy solidification experiment in TEM 01-3M facility aboard MAXUS 8. *Materials Science Forum*. **Vol. 649**, 223-228.
  11. McFadden S. and Browne D. (2009). A combined experimental-model approach to estimate the solidification macrostructures formed during a microgravity experiment on Ti-Al based intermetallic alloys. In *Proceedings of the Modeling of Casting, Welding, and Advanced Solidification Processes – XII*. Canada.
  12. Noepfel A., Budenkova O., Zimmermann G., Sturz L., Mangelinck-Noël N., Jung H., Nguyen-Thi H., Billia B., Gandin C.-A., Fautrelle Y. (2009). Numerical modeling of columnar to equiaxed transition - application to microgravity experiments. *International Journal of Cast Metals Research*. **Vol. 22**, N1-4, 34-38(5).
  13. Kartavykh A., Ginkin V., Ganina S., Rex S., Hecht U., Schmitz B., Voss D. (2011). Convection-induced peritectic macro-segregation proceeding at the directional solidification of Ti-46Al-8Nb intermetallic alloy. *Materials Chemistry and Physics*. **Vol. 126**, 200-206.